Carbon nanotubes might improve neuronal performance by favouring electrical shortcuts

Article *in* Nature Nanotechnology · March 2009

DOI: 10.1038/nnano.2008.374 · Source: PubMed

15 authors, including:

Giada Cellot
Scuola Internazionale Superiore di Studi Avanzati di Trieste
32 PUBLICATIONS **1,694** CITATIONS

SEE PROFILE

Vladimir Rancic
University of Alberta
41 PUBLICATIONS **720** CITATIONS

SEE PROFILE

Silvia Giordani
Dublin City University
139 PUBLICATIONS **6,791** CITATIONS

SEE PROFILE

nature nanotechnology

ARTICLES

PUBLISHED ONLINE: 21 DECEMBER 2008 | DOI: 10.1038/NNANO.2008.374

Carbon nanotubes might improve neuronal performance by favouring electrical shortcuts

Giada Cellot[1], Emanuele Cilia[1†], Sara Cipollone[2], Vladimir Rancic[1], Antonella Sucapane[1], Silvia Giordani[2†], Luca Gambazzi[3], Henry Markram[3], Micaela Grandolfo[4], Denis Scaini[5], Fabrizio Gelain[6], Loredana Casalis[5], Maurizio Prato[2], Michele Giugliano[3,7‡] and Laura Ballerini[1‡*]

Carbon nanotubes have been applied in several areas of nerve tissue engineering to probe and augment cell behaviour, to label and track subcellular components, and to study the growth and organization of neural networks. Recent reports show that nanotubes can sustain and promote neuronal electrical activity in networks of cultured cells, but the ways in which they affect cellular function are still poorly understood. Here, we show, using single-cell electrophysiology techniques, electron microscopy analysis and theoretical modelling, that nanotubes improve the responsiveness of neurons by forming tight contacts with the cell membranes that might favour electrical shortcuts between the proximal and distal compartments of the neuron. We propose the 'electrotonic hypothesis' to explain the physical interactions between the cell and nanotube, and the mechanisms of how carbon nanotubes might affect the collective electrical activity of cultured neuronal networks. These considerations offer a perspective that would allow us to predict or engineer interactions between neurons and carbon nanotubes.

Nanomaterials can be engineered and integrated into biological systems to form useful multifunctional devices[1–3]. Carbon nanotubes, in particular, with their intriguing chemical and physical properties[4], are promising materials for electronics, aerospace and biomedical applications[5–7]. The application of nanotubes to the central nervous system is particularly suited in at least four areas of interest in nerve-tissue engineering: probing cell behaviour, augmenting cell behaviour, labelling/tracking subcellular components and providing tissue matrix enhancement[1,6,8,9].

Because of their organized fractal-like nanostructure and high electrical conductivity, carbon nanotubes are promising materials for developing neural prosthesis[10]. They can organize into bundles that mimic neural processes[7], and have been patterned on surfaces for studying the growth and organization of neural networks[6].

Recent work shows that carbon nanotube anchored on planar substrates can promote cell attachment, growth, differentiation and long-term survival of neurons[11–15]. Furthermore, the neuron–nanotube interaction depends on the purity and three-dimensional organization of the nanotubes[15]. We have shown previously[10,14] that neurons grown on a conductive nanotube meshwork always display more efficient signal transmission. We now ask whether this efficiency is linked to the nanoscale physical interactions between the nanotube and neuron.

Here, we show by single-cell electrophysiology that direct nanotubes–substrate interactions with membranes of neurons can affect single cell activity. Neurons normally propagate electrical signals, known as action potential, down an axon. Action potentials might occasionally backpropagate to dendrites, that is against the direction flow. The interactions with nanotubes favour backpropagation of the action potential. The backpropagating current induces a voltage change that increases the concentration of Ca^{2+} in the dendrites—an event known as calcium electrogenesis—and can be measured through the presence of a slow membrane depolarization following repetitive action potentials[16]. Our results provide a new mechanistic insight into how nanotubes target the integrative properties of neurons. We further propose a mathematical model to explain the phenomena and consequences for the enhanced signal transmission[10,14] of neurons cultured on nanotube substrates.

Carbon nanotubes and electrogenesis in neurons

Functionalized single-wall or multi-wall carbon nanotubes (hereafter collectively called nanotubes unless specified) were deposited on a glass substrate and subsequently defunctionalized by thermal treatment to form glass slides covered with a purified and mechanically stable thin film (that is, a nano-meshwork) of about 50–70 nm (see Methods)[10,14]. Scanning tunnelling microscopy (STM) conductivity measurements revealed that both nanotube layers act as a largely resistive network, confirming our previous observations[10]. This is consistent with STM images that show a dense meshwork of nanotubes with a typically large surface roughness (see Supplementary Information, Fig. S1) and this suggests that long-range electrical connectivity is permitted[17].

The effect of nanotubes on neuronal integrative properties was investigated by comparing the electrophysiology of rat hippocampal cells cultured on control substrates to those grown on a thin film of purified nanotubes for 8 to 12 days. In a sample of cultures ($n = 19$) grown on nanotubes we quantified in terms of post-synaptic currents frequency (see Methods) the presence of a significant increase in synaptic activity, compared to control

[1]Life Science Department, B.R.A.I.N., University of Trieste, via Fleming 22, I-34127, Trieste, Italy, [2]Department of Pharmaceutical Sciences, University of Trieste, Piazzale Europa 1, I-34127, Trieste, Italy, [3]Laboratory of Neural Microcircuitry, Brain Mind Institute, Ecole Polytechnique Fédérale de Lausanne, Station 15, CH-1015 Lausanne, Switzerland, [4]Neurobiology Sector, International School for Advanced Studies (SISSA), via Beirut 2–4, 34014 Trieste, Italy, [5]ELETTRA Sincrotrone Trieste Strada Statale 14, Basovizza, Trieste, Italy, [6]Biosciences and Biotechnology Department, University of Milan-Bicocca, Piazza della Scienza 2, 20126 Milan, Italy, [7]Department of Biomedical Sciences, University of Antwerp, Universiteitsplein 1, B-2610 Wilrijk, Belgium; [†]Present address: Department of Biomedical Science, University of Antwerp, Universiteitsplein 1, B-2610 Wilrijk, Belgium (E.C.); School of Chemistry, Trinity College, Dublin College Green, Dublin 2, Ireland (S.G.); [‡]These authors contributed equally to this work; *e-mail: ballerin@psico.units.it

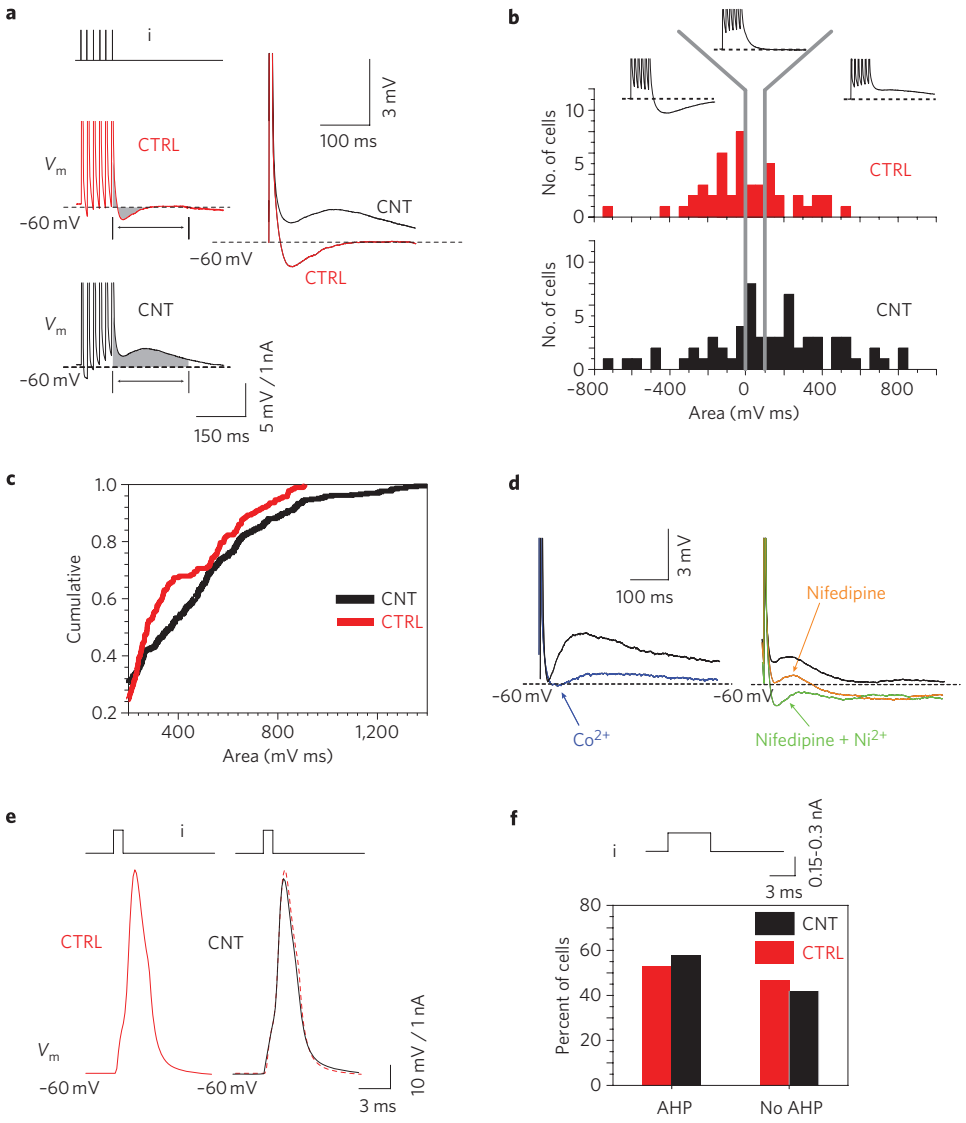

Figure 1 | The effect of nanotubes (CNTs) on neuronal excitability. a, The nanotube induced significantly larger after-potential depolarization (ADP) following a spike-train. Current pulses at 80 Hz (upper trace) evoke precisely timed action potentials in control (CTRL) and nanotubes (CNT; left). Averaged voltage trajectories V_m are superimposed for comparison (right). Areas below the voltage traces (grey shading) are quantified over 100 ms, 50 ms after (arrow) the last action potential. The relative magnitude of the area defines hyperpolarizing (AHP), neutral (NR) and ADP responses. **b**, Area distributions summary ($n = 48$ CTRL, $n = 66$ CNT, respectively). **c**, Relative cumulative frequency distributions of ADP area values in neurons grown on nanotubes ($n = 394$) and in control ($n = 187$). Note the significant ($P < 0.005$) increase in the proportion of larger-amplitude ADPs compared to those in control neurons. **d**, Pharmacological blockade of calcium channels removed the ADP, even unmasking an AHP. **e**, Evoked single spikes show similar amplitude and shape in the two growth conditions, generally showing AHP or NR. The red dashed line is identical to the CTRL spike and it is added to facilitate the visual comparison. **f**, After-potentials were also quantified as in **a**, pooling together results obtained with 4 and 10 ms current step duration, revealing no difference between control and nanotubes.

cultures. This increased activity represents a typical feature of neurons grown on nanotube substrates[10,14]. After this initial assessment, all recordings were conducted in the presence of 10 μM 6-cyano-7-nitroquinoxaline-2,3-dione (CNQX) and 5 μM gabazine (SR-95531), resulting in synaptic decoupling of individual neurons from each other. These chemical blockers selectively suppressed network activity while leaving endogenous neuronal excitability unaffected, allowing us to investigate electrogenesis in isolated neurons.

We studied the contribution of nanotubes to neuronal electrical regenerative properties by whole-cell current-clamp recordings from single neurons ($n = 64$ and $n = 82$, control and nanotubes, respectively). In the first set of experiments we used a standard stimulation protocol[16] to probe the regenerative and excitable properties in the proximal and distal compartments of the neuron. Injecting a brief current pulse into the soma (4 ms, 1 nA), we forced the neuron to fire a regular train of six action potentials at frequencies ranging from 20 to 100 Hz (Fig. 1a, top). We addressed the effects of the nanotubes on the integrative properties of the neurons by investigating the presence of additional somatic membrane depolarization after the last action potential of the train. Such an after-depolarization (ADP) represents an indirect effect of dendritic Ca^{2+} electrogenesis, which is dependent on the coupling between the soma and dendrites[18,19] and is mediated by backpropagating action potentials[16]. We computed the area under the trace in a 100 ms time window, starting at 50 ms after the last action potential of the train, taking the resting membrane potential as a reference. Figure 1a (left) shows an example of such recordings

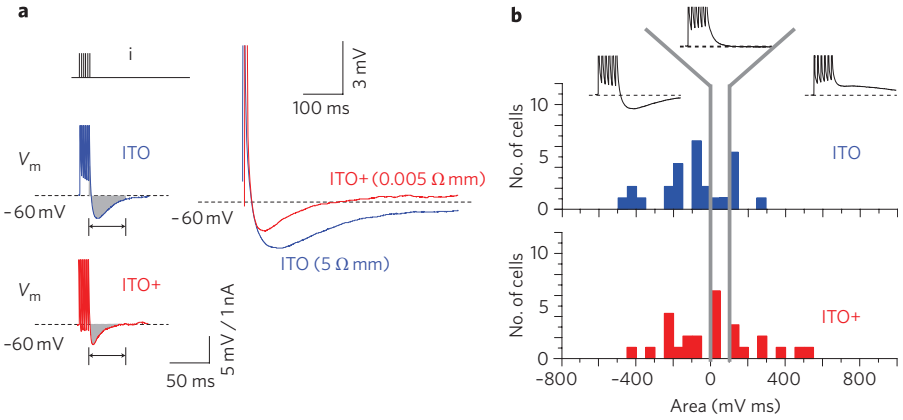

Figure 2 | Planar electrically conductive surfaces do not affect after-potential neuronal excitability. An excellent conductor, indium tin oxide (ITO), sputtered on glass coverslips and used as a smooth growth substrate, did not induce ADP. **a**, Voltage trajectories after stimulation with a spike-train. Cells grown on ITO substrates with normal (ITO, $n = 26$) and increased conductibility (ITO+, $n = 27$) were similar to control. **b**, However, the ITO population summaries show significantly different distribution profiles compared to nanotubes (compare with Fig. 1b).

(80 Hz). Note the presence of the depolarizing after-potential in the presence of nanotubes.

We classified after-potential responses into three categories based on area values: after hyperpolarization (AHP, area < 0 mV ms), neutral response (NR, $0 >$ area < 100 mV ms) and after depolarization (ADP, area > 100 mV ms). Figure 1b reports the distribution of these responses in control and nanotubes substrates. The majority (72%) of control neurons lying on glass substrates, when forced to fire action potentials trains, displayed either an AHP (47%) or NR (25%). ADP was observed only in a subset of cells (28%, Fig. 1a,b,c; $n = 48$). Conversely, 54% of neurons grown on nanotubes displayed an ADP response (Fig. 1a,b; $n = 66$), with AHP in 28% of recorded cells and NR in 18%.

A direct comparison of ADP effects measured in control or in nanotubes neurons (Fig. 1c), revealed that the frequency distribution of ADP values was significantly shifted to the right ($P < 0.005$) in nanotubes systems, indicating an increase in the proportion of larger-amplitude ADP when compared to control. This showed that nanotube neurons have a higher probability of generating an ADP upon firing a train of action potentials and the ADP areas are larger than those detected in the control. Such an ADP might reflect dendritic Ca^{2+}-dependent electrogenesis[19]. Consistent with this hypothesis, ADP was abolished when bathed with 3 mM $CoCl_2$, a non-specific voltage-gated Ca^{2+}channel blocker ($n = 3$; Fig. 1d, left). ADP could be blocked in part by 10 μM nifedipine and further abolished by co-application of 50 μM $NiCl_2$ (Fig. 1d, right; $n = 10$). These results indicated that the ADP was generated by both high and low voltage-activated Ca^{2+}channels[20]. Applications of the same blockers in control neurons displaying AHP, highly increased (by $500 \pm 113\%$) the hyperpolarization ($n = 6$; not shown).

Action potentials, evoked by single current pulses, displayed comparable shape and amplitude in both groups (control 116 ± 3 mV, $n = 48$, and nanotubes 111 ± 2 mV, $n = 66$; Fig. 1e)[10,14]. We observed no differences between the two groups in single action potential after-potentials, known to regulate intrinsic repetitive firing[21]. Firing was also induced using longer (10 ms, 0.15–0.3 nA, $n = 38$) depolarizing current steps and the AHP quantified[21]. Figure 1f summarizes the probability of finding cells generating an AHP: no differences between the two groups were observed. We conclude that integration of a train of action potentials, not a single spike, is required for the ADP to appear, reminiscent of the occurrence of electrotonic summation of (back)propagating action potentials in distal neuronal compartments[22].

Testing the dendritic origin of the ADP, we also recorded responses to a train of action potentials in a different class of cultured neurons, the dorsal root ganglion cells. These neurons are considerably different from hippocampal neurons in that they have little to no dendritic arborization. When ganglion neurons were tested they never displayed ADP at any of the spike frequencies tested (20–100 Hz, $n = 35$; data not shown).

Effect of conductivity and nanoscale features on neurons

Nanotubes substrates are electrically conductive and feature a nanoscale meshwork. In order to clarify whether both these physical properties are linked to ADP generation, hippocampal neurons were also cultured on two other substrate types: (a) indium tin oxide (ITO), characterized by high electrical conductivity in the absence of surface nano-roughness[23] and (b) RADA16 (Ac– RADARADARADARADA–$COHN_2$) peptides characterized by the absence of conductivity in the presence of a clear nanoscale scaffold[24].

We used two different ITO coverslips having different resistance ranges: one with resistivity values (5 Ω mm) comparable to nanotubes coverslips (1–1.2 Ω mm) and a second one with a lower resistivity (0.005 Ω mm). Neurons attached and grew on ITO, similarly to controls on glass. The majority (79%; Fig. 2a,b; $n = 53$) of ITO neurons displayed AHP or NR responses following stimulation, whereas only 21% of recorded cells underwent ADP. No correlation was observed with respect to the substrate resistance.

RADA16 peptide substrates were layered on glass coverslips and self-assembled into nanofibres as shown by AFM (Fig. 3a,b). Cultured neurons grew on the substrate (Fig. 3b,c), which had a local nano-meshwork similar to nanotube substrates (Fig. 3c) but without the conductive properties of the nanotubes. Neurons cultured on RADA16 displayed similar passive properties to those on control and nanotube substrates (summarized in Fig. 3d, plots are for all conditions). When tested, RADA16 neurons replicated the control and ITO response profile, displaying in the majority of cases AHP or NR responses (72.5%; Fig. 3c; $n = 40$), with only 27.5% of neurons undergoing ADP. These results showed that the effects of nanotube layers on neuronal behaviour are specific and not simply reproducible by any substrate displaying either high conductivity or a clear nanostructure.

The electrotonic hypothesis

Biophysical descriptions of neuronal excitability can be reduced to simple two–compartment morphologies[18,25] (Fig. 4c,d) that can still represent dendritic calcium electrogenesis and backpropagating action potentials. Here, we further simplified a ball-and-stick neuron to a fully passive electric circuit (Fig. 4a,b). Somatic action

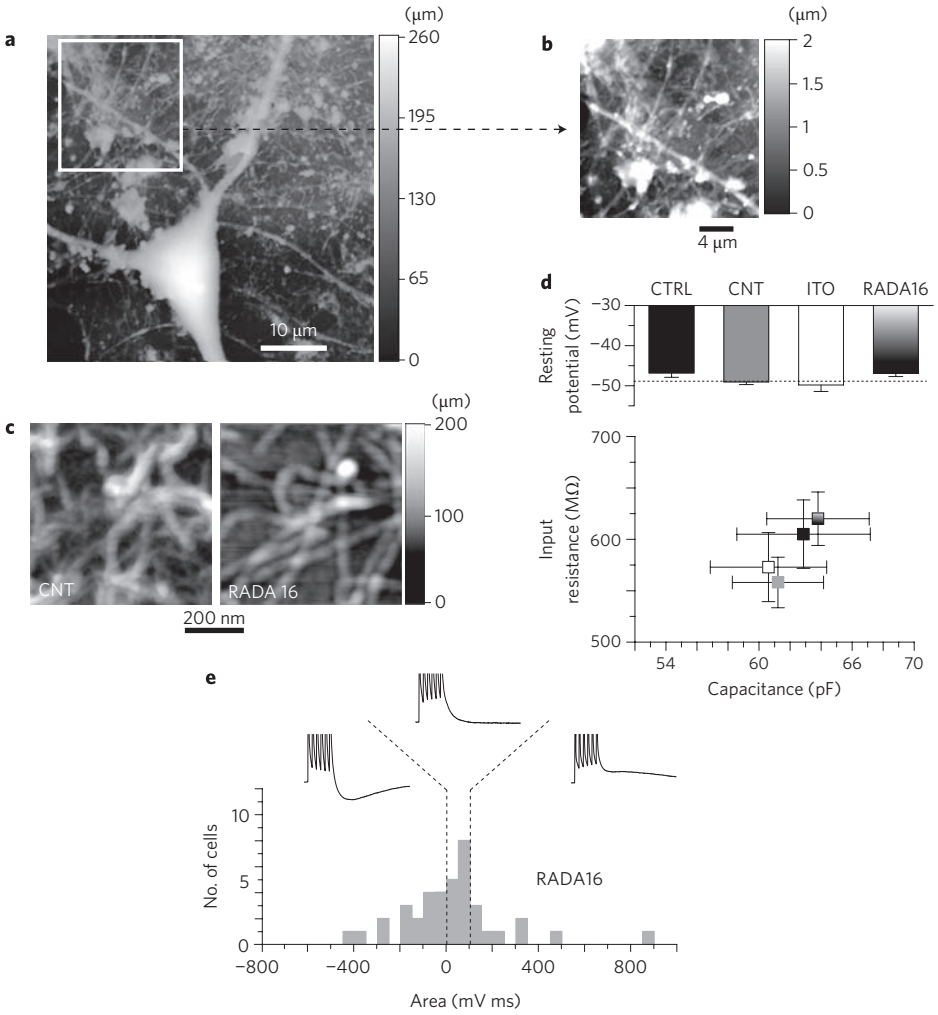

Figure 3 | Effect of conductivity and nanoscale features on neurons. a–c, AFM shows that RADA16 peptides form scaffolds similar to nanotubes (CNT) and cells grow well on them without any effect on after-potential excitability. **d**, Passive properties of the membranes of neurons grown on glass control (CTRL), nanotubes (CNT), indium tin oxide (ITO) or RADA16 peptides (RADA16) are comparable at their resting potential. **e**, Population summary ($n = 40$), as in Fig. 1a, showed no significant difference compared to control.

potentials were modelled as stereotyped waveforms of an ideal generator V_s. During a spike, the membrane voltage V_d at a (distal) dendritic location was therefore an attenuated replica of V_s, as in voltage dividers[26]. Considering conductive nanoscopic substrates with the unusually tight mechanical proximity with the cellular membrane (that is, 'pinching' in the extreme case; Fig. 4a)[10], we investigated whether an electrotonic shortcut between the soma and dendrite may occur. This would effectively turn distal electrical compartments into proximal ones, with respect to the soma. Although far from being proved, this hypothesis is the simplest to account for the extra depolarization accumulated in dendritic compartments after a train of action potentials. We further assumed that the tight neuron–substrate adhesion occurs at discontinuous points (see Fig. 5c), at least in correspondence with somatic and (distal) dendritic membranes.

In the case of an electrically conductive substrate, and for fast action potential waveforms, one can model the substrate–electrolyte interface with a parallel arrangement of a capacitor and a resistor[27], capturing both coupling phenomena. This holds for both the substrate–electrolyte junction and the substrate–cytosol junction, where the membrane is pinched and the substrate becomes in part intracellularly exposed. Such a scenario (Fig. 4b) was studied by analysing an input–output relationship between V_s and V_d (ref. 26).

In a regime of slowly varying neuronal signals, the boosting effect of the substrate in a soma-to-dendrite coupling will occur only if $R_0 < R < R_0(R_a/R_d)$. Because we expect $R > R_0$, as they inversely depend on the exposed surface (that is, $S < S_0$), the previous inequality can be satisfied for $R_a \gg R_d$, as in the case of very distal dendrites. On the other hand, in the regime of quickly varying signals, for example the action potential itself, boosting may occur when $C_0(R_d/R_a) < C < C_0$, obtained under the assumption $R = \infty$. Similarly, this condition might be satisfied for $R_d \ll R_a$, which refers again to distal dendritic compartments. This conclusion, which assumes boosting only during fast repetitive variation in neuronal signals, is supported by the absence of changes brought about by nanotubes in the dendritic passive time constants, in both DRG and hippocampal neurons (see Supplementary Information).

Alternative theories to account for the increased effects of ADP might involve a potentiation of calcium-mediated currents occurring in neurons growing on nanotubes. Channels clustering, induced by mechanical interactions between nanotubes bundles and the cell cytoskeleton, might equally account for the observed ADP. Nevertheless, the formation of such 'hot-spots' for calcium currents should be limited to distal dendritic compartments, assuming that mechanical interactions between the nanotubes and the cytoskeleton might be more apparent at the small-diameter neuronal branches. Along these lines, one can also propose that both mechanical and

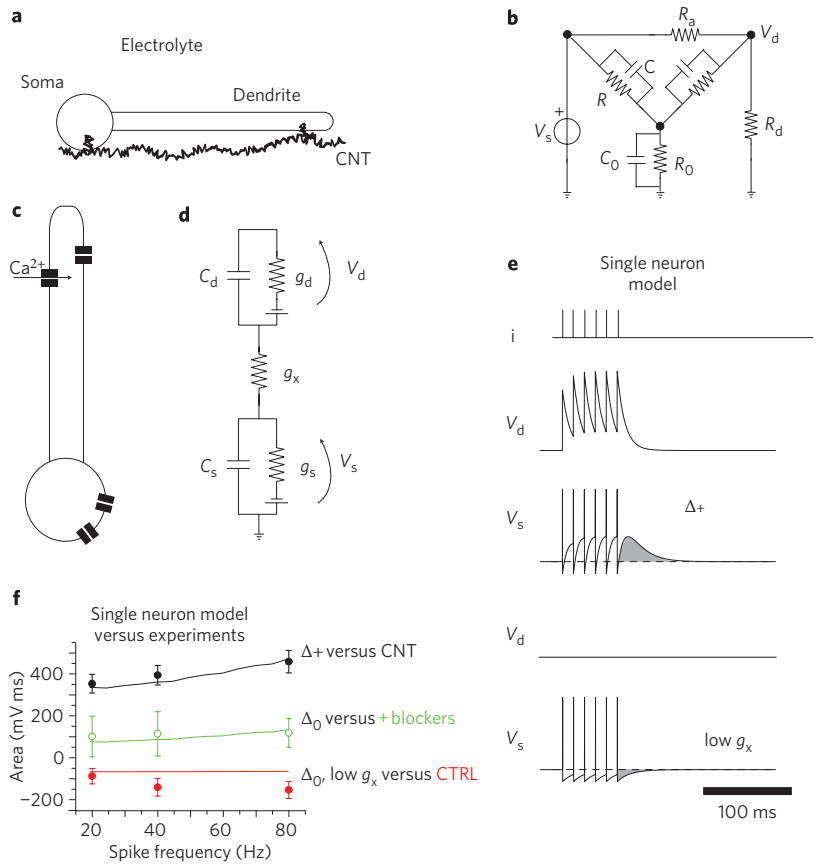

Figure 4 | The electrotonic hypothesis. a, Intracellular compartments are electrically exposed to bundles of substrate nanotubes and such contacts might result in an electrical shortcut (summarized with an equivalent electric circuit model). **b**, The cell soma acts as a generator V_s during a spike, the somato-dendritic attenuation is modelled by a resistor R_a, and the shunting effect of the bulk electrolyte is represented by an R_0–C_0 parallel arrangement[27]. The intracellular interface nanotube–electrolyte is also represented by an R–C parallel arrangement. This circuit model allows us to analyse the physical conditions that might underlie the nanotube-mediated boosting effect of the somato-dendritic coupling. **c,d**, A two-compartment spiking neuron model (see Supplementary Information) was used to reproduce CNT-induced ADP and to investigate its consequences in a neuronal network. **e**, Model parameters can be tuned to replicate some of the single-neuron properties observed experimentally (see Fig. 1a). **f**, Simulated responses (continuous lines) are compared to the weak frequency dependence of ADP ($n = 28$ cells on nanotubes; black circles) and AHP ($n = 19$ cells on control glass; red circles. ADP in cells grown on nanotubes ($n = 8$) had a strong sensitivity to calcium channel blockers (green circles).

electrical interactions of the nanotubes lead to the formation of calcium channel clusters for which the voltage gating is directly affected by the local electric field of the nanotubes. It is certainly possible, although unlikely, that metal particles and other impurities in the nanotubes substrates resulting from the deposition and purification processes[28] might alter the electrical properties of the neurons. Although we do not have any clear-cut evidence to (dis)prove each of the hypotheses discussed so far, we have evidence that neurons, such as ganglion cells, that are characterized by a completely different dendritic morphology *in vitro*, behave as those grown on control substrates. The existence of an unspecific 'toxic' effect of nanotubes on the cells is therefore unlikely.

Morphological evidence for the electrotonic hypothesis

We investigated the presence of discontinuous and tight interactions between nanotubes and neuronal membrane by transmission electron microscopy (TEM). Planar sections of the morphology and organization of hippocampal cells grown on nanotubes are shown in Fig. 5a. Note the presence of synaptic contacts, mitochondria and ribosomes, together with clearly distinguishable longitudinal neurite sections containing bundles of microfilaments. In addition, in this section, a presumed glial cell is identified by the typical electron density of the cytoplasm (labelled G, Fig. 5a, right)[29]. All these features are indicative of healthy cultures.

The same sample was further analysed in sagittal sections to visualize the zone of nanotubes–membrane contact, as shown in Fig. 5b,c. Note the recurrent, discontinuous and tight contact between the nanotubes and the neuronal membrane. In this sample we used multi-wall nanotubes, clearly recognizable by their typical TEM aspect[30] (Fig. 5d). Multi-wall nanotubes, in clear continuity with the nanotubes meshwork outside the neuron (Fig. 5c,e), are in intimate contact with a small area of the neuritic membranes (Fig. 5c,e,f). These ultra structural interactions between nanotubes and neuronal membranes were observed in all sections explored (Fig. 5f), supporting the hypothesis that intimate discontinuous interactions of nanotubes with neuronal membrane surfaces can induce specific changes in membrane electrical behaviour.

Modelling the impact of nanotubes on neuronal activity

Here, we introduce our modelling strategy to predict the impact of nanotube-induced neuronal potentiation on neuronal circuit activity. We extended the model of Fig. 4b to a two-compartment integrate-and-fire neuron (Fig. 4c) to simulate how nanotubes-induced ADP might affect network activity. Once the model parameters corresponding to the amplitude of the backpropagating action potential (Δ) and to the somatodendritic electric coupling (g_x; that is, the ADP) were tuned to replicate the experimental

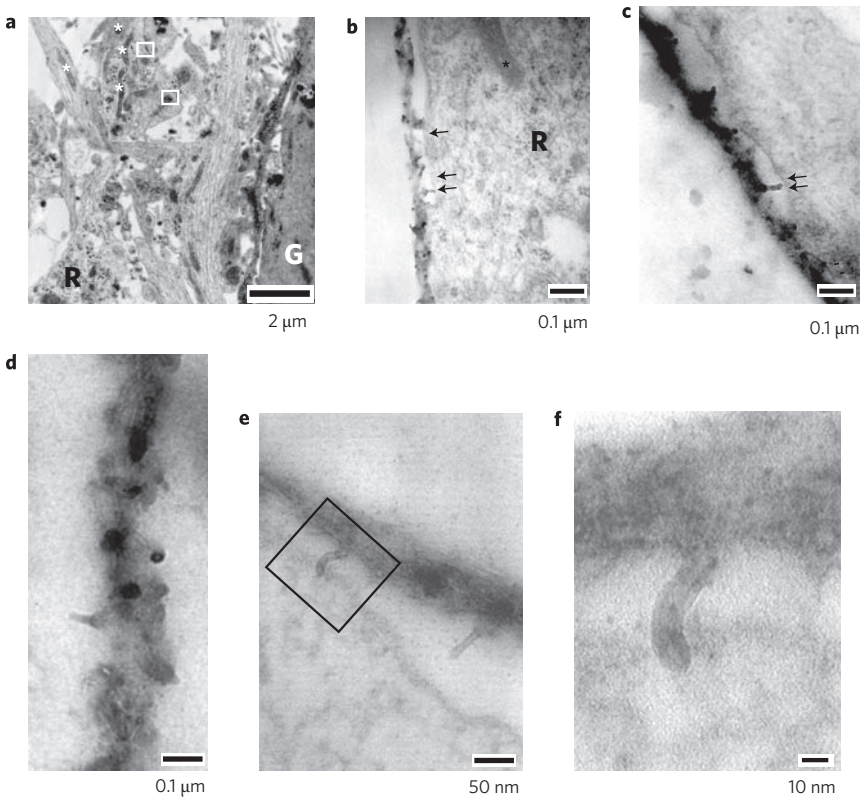

Figure 5 | The ultrastructural interaction between multi-wall nanotubes and neurons. a, TEM planar sections of neurons grown on nanotubes show a healthy organization of neuronal networks, accompanied by the presence of synaptic contacts (rectangular boxes). The asterisk indicates mitochondria and R indicates clusters of ribosomes. Longitudinal sections of neurites containing microfilaments are clearly distinguishable. A portion of a presumed glial cell is indicated by 'G', identifiable by the intense electron density of its cytoplasm. **b,c**, TEM sagittal sections illustrate multi-wall nanotubes–membrane contacts, indicated by arrows. **d**, Morphology of nanotubes. **e,f**, High-magnification micrographs from a section consecutive to those of **b** and **c**. The rectangular area in **e** is magnified in **f**. Note how nanotubes are 'pinching' neuronal membranes.

observations (compare Fig. 4e to Fig. 1a; see also Fig. 4f), a small-sized recurrent network of model neurons was simulated (see Supplementary Information, Methods). In such a modelled network of neurons, spontaneous neuronal activity emerges as irregular synchronized firing epochs[10,14] or bursts. When we added the additional ADP induced by nanotubes in the simulated neurons, this did not increase the network activity (Fig. 6a); instead, it significantly prolonged the duration of bursts (Fig. 6a, inset) in the simulated network. Prolonged epochs of burst firing were indirectly evaluated experimentally by monitoring postsynaptic currents in single neurons (Fig. 6b). We used each voltage-clamped cell as a probe to sense presynaptic network activity. When control and nanotubes postsynaptic currents were aligned to the time of crossing a detection threshold and then averaged (see Supplementary Information, Methods), the resulting waveform durations indicated that the probability of presynaptic events clustering was much higher in nanotubes cultures ($n = 3$) compared to control cultures ($n = 3$) (Fig. 6b). Quantitative differences in the postsynaptic currents duration ($n = 785$, nanotubes; $n = 413$, control) were quantified as area values and found statistically significant ($P < 0.05$), as is apparent from their distributions (Fig. 6c). We speculate that a prolonged duration of correlated firing across the network might ultimately potentiate synaptic interactions[31]. Such an increase in synaptic efficacy would in turn result in an increased frequency in burst firing[32].

We propose that, due to the interaction among nanotubes and neurons, the efficacy in action potential backpropagation is enhanced; thus nanotubes reengineer neuronal integrative properties *in vitro*. The presence of the ADPs, their dependence on trains of action potentials together with the detected sensitivity to calcium channel blockers, in particular Ni^{2+} sensitivity, given that Ni^{2+}-sensitive channels are typically expressed at high density in distal dendrites[33,34], are all indicative of the generation of dendritic Ca^{2+} currents[16,19,35]. This hypothesis, replicated and grounded by mathematical modelling, is strengthened by the lack of difference in afterpotentials when single spikes are elicited in control or in nanotubes neurons.

The precise mechanisms for the observed effect of nanotubes substrates in this study are not yet totally clear. Our TEM results suggest that one mechanism might rely on the detected discontinuous and tight contact between nanotubes and membranes. The morphology of such contacts is indicative of the development of hybrid nanotubes–neuronal units. Are these units functionally different from other membrane areas? We put forward a provocative interpretation where a direct resistive and capacitive coupling between nanotubes and fast repetitive voltage signals generated by neurons is enhanced at these areas, leading to reinforcement of signalling, more effective at distal dendrites. Alternatively, such hybrid areas might be characterized by a nanotubes-induced clustering of calcium channels. Although we cannot exclude this possibility, the lack of changes in afterpotentials following a single action potential or after trains of action potentials in the ganglion cell experiments do not fully support this interpretation, because such an increased density in calcium channels should be distributed in all neuronal compartments, regardless of dendrite complexity. Other morphological modifications induced by the nanotubes substrates might certainly have an impact on backpropagation of action potentials, although significant changes in the passive neuronal membrane properties could be ruled out.

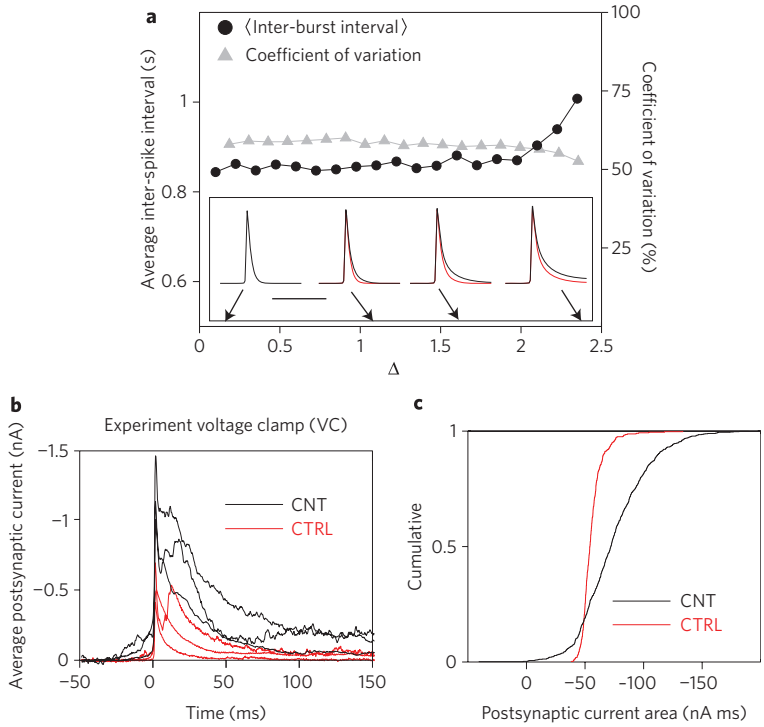

Figure 6 | Network-level correlate of ADP in single neurons: model and experiment. Irregular bursts of activity emerge in the mean firing rate of recurrent networks of model neurons (see Supplementary information). **a**, The somato-dendritic coupling of individual model neurons (see Fig. 4e and f) does not affect the mean inter-burst interval and variability. The duration of each burst increases with increased coupling (inset, calibration 100 ms). **b**, This was indeed observed in the experiments, where the average spontaneous postsynaptic currents waveforms in six neurons were computed to provide a measure of the probability of presynaptic event clustering (that is, a burst of spikes), within a window of 50–150 ms around its peak. **c**, Significant differences in the postsynaptic currents duration are apparent from the shift in the empirical cumulative distributions of their areas.

Despite these considerations on hypothetical mechanisms, the results reported here indicate that nanotubes might affect neuronal information processing. It is tempting to speculate that gaining insights into the functioning of hybrid neuronal/nanotubes networks might be relevant for the design of smart materials, triggering specific synaptic reorganization in a neuronal network. Although simplified, to our knowledge these considerations represent the first attempt at linking electrical phenomena in nanomaterials to neuronal excitability and may allow one to predict or engineer the interactions between nanomaterials and neurons.

Methods

Purification of nanotubes, RADA16 and deposition onto glass coverslips. The nanotubes (HiPCO nanotubes, Carbon Nanotechnology) were functionalized by means of a 1,3-dipolar cycloaddition reaction[10,14,28], in dimethylformamide (DMF), between sarcosine, heptanal and purified single-wall or multi-wall nanotubes. After reaction, the nanotubes were filtered on a polytetrafluoroethylene (PTFE) membrane and extensively washed with DMF and dichloromethane. For deposition on the coverslips, functionalized nanotubes were resuspended in fresh DMF (by ultrasonic bath), and a few drops of the solution were deposited on the glass slides. After slow evaporation of DMF (100 °C), the glass coverslips were annealed at 350 °C under nitrogen for 20 min. This process permits defunctionalization of the nanotubes and fixes them onto the glass surface.

The resistivity of the single-wall and multi-wall nanotubes deposition was estimated to be 1.0–1.2 Ω mm and 10–20 Ω mm, respectively, calculated by the four-wire measurement technique and a Precision Impedance Analyzer (4294A, Agilent Technology). STM images in the Supplementary Information, Fig. S1, show the dense meshwork formed by nanotubes. In both cases, single-wall and multi-wall nanotubes depositions displayed a uniform cross-section thickness of around 50–70 nm, estimated by SEM investigations using a focused ion beam technique (not shown) and by TEM sagittal sections analysis (Fig. 5c).

All scanning probe measurements were carried out using a commercial NT-MDT Solver Pro atomic force microscopy (AFM) endowed with a current amplifier (AU006 from NT-MDT Co.) capable of measuring currents through conductive cantilevers. AFM characterization of the surfaces was carried out in semicontact mode using high-resolution silicon cantilevers (μmasch HiRes-W/AlBS, spring constant 5 nN nm^{-1}, apex radius of about 1 nm). STM measurements were accomplished using the same equipment but setting the feedback in current and using a conductive, platinum-covered, AFM tip as probe (μmasch CSC21/Ti-Pt, spring constant 2 nN nm^{-1}).

RADA16 peptide (courtesy of Dr F. Gelain) was diluted to a final concentration of 10 mg ml^{-1} (1% w/v) in sterile water for tissue culture; a drop (100 μl) of this solution was layered on clean and sterile coverslips, left to dry at +37 °C and rinsed once with sterile distilled water.

Industrial-quality ITO substrates (Multichannel Systems) were obtained by depositing a thin conductive layer of ITO on glass substrates. Because of its low electrical resistance (0.005–5 Ω mm), we used ITO substrates as a cell culture smooth substrate, forming the alternative to nanotubes.

Tissue cultures and electrophysiology. Standard dissociated hippocampal cultures (188 series) were prepared according to Lovat and colleagues[14] and whole-cell patch-clamp recordings were obtained at room temperature from the soma of neurons (see Supplementary Information, Methods). Neuronal passive properties of cells grown on nanotubes layers were quantified and compared with those grown under control conditions. The resting membrane potential (r.m.p.) did not significantly differ between the two groups (-47 ± 1 mV, $n = 52$, controls; -49 ± 1 mV, $n = 72$, nanotubes). Similarly, we detected no differences in input resistance (R_{IN}) and the cell capacitance values (control, 605 ± 33 MΩ, 63 ± 4 pF, $n = 52$; nanotubes, 558 ± 24 MΩ, 61 ± 3 pF, $n = 72$, summarized in Fig. 3d). We performed a similar analysis on neurons grown on ITO or RADA16 substrates. In both groups r.m.p. (ITO, 50 ± 2, $n = 15$; RADA16, 47 ± 1, $n = 40$), R_{IN}, and membrane capacitance (ITO, 573 ± 33 MΩ, 61 ± 4 pF, $n = 33$; RADA16, 620 ± 26 MΩ, 63 ± 4 pF, $n = 40$) displayed comparable values to those measured using nanotubes or controls (summarized in Fig. 3d).

Hippocampal neurons, grown on nanotubes or on control glass substrates, displayed prominent spontaneous electrical activity after the first days in culture[10,14]. On average, 100–400 spontaneous postsynaptic currents were analysed from each cell. Under the voltage-clamp configuration, a typical[10,14] strong increase in the occurrence of postsynaptic currents (from 0.7 ± 0.2 Hz to 1.7 ± 0.4 Hz, $n = 19$ cells) was observed in neurons grown on nanotubes when compared to controls.

In current-clamp experiments neurons of similar size, grown on control, nanotubes, ITO or RADA16 substrates, were held at −60 mV (0.014–0.021 nA, steady-state current). Trains of brief positive current pulses (1 nA, 4 ms) were injected into the soma of patched neurons to evoke precisely timed action potentials at 20–100 Hz, while monitoring the trajectory of the membrane potential following

the last action potential of the train. The APD (hyperpolarization) was quantified over a window of 100 ms by calculating the area below (above) the voltage trace, 50 ms after the time of the last action potential, referred to the resting membrane potential[16].

Received 22 September 2008; accepted 17 November 2008; published online 21 December 2008

References

1. Silva, G. A. Neuroscience nanotechnology: progress, opportunities and challenges. *Nature Rev. Neurosci.* **7,** 65–74 (2006).
2. Silva, G. A. Nanotechnology approaches for drug and small molecule delivery across the blood brain barrier. *Surg. Neurol.* **67,** 113–116 (2007).
3. Fortina, P., Kricka, L. J., Surrey, S. & Grodzinski, P. Nanobiotechnology: the promise and reality of new approaches to molecular recognition. *Trends Biotechnol.* **23,** 168–173 (2005).
4. Parpura, V. Instrumentation: carbon nanotubes on the brain. *Nature Nanotech.* **3,** 384–385 (2008).
5. Krishnan, A., Dujardin, E., Ebbesen, T. W., Yianilos, P. N. & Treacy, M. M. J. Young's modulus of single-walled nanotubes. *Phys. Rev. B* **58,** 14013–14019 (1998).
6. Harrison, B. S. & Atala, A. Carbon nanotube applications for tissue engineering. *Biomaterials* **28,** 344–353 (2007).
7. Giugliano, M., Prato, M. & Ballerini, L. Nanomaterial/neuronal hybrid system for functional recovery of the CNS. *Drug Discov. Today: Disease Models*, doi: 10.1016/j.ddmod.2008.07.004 (2008).
8. Keefer, E. W., Botterman, B. R., Romero, M. I., Rossi, A. F. & Gross, G. W. Carbon nanotube coating improves neuronal recordings. *Nature Nanotech.* **3,** 434–439 (2008).
9. Ballerini, L. Bridging multiple levels of exploration: towards a neuroengineering-based approach to physiological and pathological problems in neuroscience. *Frontiers Neurosci.* **2,** 24–25 (2008).
10. Mazzatenta, A. *et al.* Interfacing neurons with carbon nanotubes: electrical signal transfer and synaptic stimulation in cultured brain circuits. *J. Neurosci.* **27,** 6931–6936 (2007).
11. Mattson, M. P., Haddon, R. C. & Rao A. M. Molecular functionalization of carbon nanotubes use as substrates for neuronal growth. *J. Mol. Neurosci.* **14,** 175–182 (2000).
12. Hu, H., Ni, Y., Montana, V., Haddon, R. C. & Parpura, V. Chemically functionalized carbon nanotubes as substrates for neuronal growth. *Nano Lett.* **4,** 507–511 (2004).
13. Hu, H. *et al.* Polyethyleneimine functionalized single-walled carbon nanotubes as a substrate for neuronal growth. *J. Phys. Chem. B* **109,** 4285–4289 (2005).
14. Lovat, V. *et al.* Carbon nanotube substrates boost neuronal electrical signaling. *Nano Lett.* **5,** 1107–1110 (2005).
15. Galvan-Garcia, P. *et al.* Robust cell migration and neuronal growth on pristine carbon nanotube sheets and yarns. *J. Biomater. Sci. Polym. Ed.* **18,** 1245–1261 (2007).
16. Schaefer, A. T., Larkum, M. E., Sakmann, B. & Roth, A. Coincidence detection in pyramidal neurons is tuned by their dendritic branching pattern. *J. Neurophysiol.* **89,** 3143–3154 (2003).
17. Kirckpatrick, S. Percolation and conduction. *Rev. Mod. Phys.* **45,** 574–588 (1972).
18. Larkum, M. E., Kaiser, K. M. & Sakmann, B. Calcium electrogenesis in distal apical dendrites of layer 5 pyramidal cells at a critical frequency of back-propagating action potentials. *Proc. Natl Acad. Sci. USA* **96,** 14600–14604 (1999).
19. Larkum, M. E., Waters, J., Sakmann, B. & Helmchen, F. Dendritic spikes in apical dendrites of neocortical layer 2/3 pyramidal neurons. *J. Neurosci.* **27,** 8999–9008 (2007).
20. Seamans, J. K., Gorelova, N. A. & Yang, C. R. Contributions of voltage-gated Ca^{2+} channels in the proximal versus distal dendrites to synaptic integration in prefrontal cortical neurons. *J. Neurosci.* **17,** 5936–5948 (1997).
21. Young, C. E. & Yang, C. R. Dopamine D1/D5 receptor modulates state-dependent switching of soma-dendritic Ca^{2+} potentials via differential protein kinase A and C activation in rat prefrontal cortical neurons. *J. Neurosci.* **24,** 8–23 (2004).
22. Markram, H., Helm, P. J. & Sakmann, B. Dendritic calcium transients evoked by single back-propagating action potentials in rat neocortical pyramidal neurons. *J. Physiol.* **485,** 1–20 (1995).
23. Nyberg, T., Shimada, A. & Torimitsu, K. Ion conducting polymer microelectrodes for interfacing with neural networks. *J. Neurosci. Methods* **160,** 16–25 (2007).
24. Gelain, F., Bottai, D., Vescovi, A. & Zhang, S. Designer self-assembling peptide nanofiber scaffolds for adult mouse neural stem cell 3-dimensional cultures. *PLoS ONE* **1,** e119 (2006).
25. Larkum, M. E., Senn, W. & Lüscher, H. R. Top-down dendritic input increases the gain of layer 5 pyramidal neurons. *Cereb. Cortex* **14,** 1059–1070 (2004).
26. Horowitz, P. & Hill, W. *The Art of Electronics* 2nd edn (Cambridge Univ. Press, 1989).
27. Robinson, D. A. The electrical properties of metal microelectrodes. *Proc. IEEE* **56,** 1065–1071 (1968).
28. Georgakilas, V. *et al.* Organic functionalization of carbon nanotubes. *J. Am. Chem. Soc.* **124,** 760–761 (2002).
29. Peters, A., Palay, S. L. & Webster, H. F. *The Fine Structure of the Nervous System* (Oxford Univ. Press, 1991).
30. Pastorin, G. *et al.* Double functionalization of carbon nanotubes for multimodal drug delivery. *Chem. Commun.* **11,** 1182–1184 (2006).
31. Markram, H., Lübke, J., Frotscher, M. & Sakmann, B. Regulation of synaptic efficacy by coincidence of postsynaptic APs and EPSPs. *Science* **275,** 213–215 (1997).
32. Giugliano, M., Darbon, P., Arsiero, M., Lüscher, H. R. & Streit, J. Single-neuron discharge properties and network activity in dissociated cultures of neocortex. *J. Neurophysiol.* **92,** 977–996 (2004).
33. Christie, B. R., Eliot, L. S., Ito, K., Miyakawa, H. & Johnston, D. Different Ca^{2+} channels in soma and dendrites of hippocampal pyramidal neurons mediate spike-induced Ca^{2+} influx. *J. Neurophysiol.* **73,** 2553–2557 (1995).
34. Magee, J. C. & Carruth, M. Dendritic voltage-gated ion channels regulate the action potential firing mode of hippocampal CA1 pyramidal neurons. *J. Neurophysiol.* **82,** 1895–1901 (1999).
35. Kampa, B. M. & Stuart, G. J. Calcium spikes in basal dendrites of layer 5 pyramidal neurons during action potential bursts. *J. Neurosci.* **26,** 7424–7432 (2006).

Acknowledgements

We are grateful to A. Roth, A. Schaefer and I. Riachi for helpful discussions, K.-H. Boven for providing ITO substrates, C. Zacchigna for assistance with tissue cultures, C. Gamboz and A. Mazzatenta for TEM procedures, and to L. Sivilotti for comments on the previous version of this manuscript. Financial support from EPFL (to M.G., L.G. and H.M.), EU (NEURONANO-NMP4-CT-2006-031847 to M.P., M.G., H.M. and L.B.), CARIPLO (to F.G.), Fondazione Alberto and Kathleen Casali, and Progetto D4 Area Science Park mobility program (to E.C.) is gratefully acknowledged.

Additional information

Supplementary Information accompanies this paper at www.nature.com/naturenanotechnology. Reprints and permission information is available online at http://npg.nature.com/reprintsandpermissions/. Correspondence and requests for materials should be addressed to L.B.